Friction **11**(6): 977–991 (2023)
https://doi.org/10.1007/s40544-022-0638-1
ISSN 2223-7690
CN 10-1237/TH
RESEARCH ARTICLE

Conductivity and tribological properties of IL-PANI/WS_2 composite material in lithium complex grease

Yanqiu XIA*, Yuanhui WANG, Chenglong HU, Xin FENG
School of Energy Power and Mechanical Engineering, North China Electric Power University, Beijing 102206, China
Received: 05 January 2022 / Revised: 01 March 2022 / Accepted: 21 April 2022

Abstract: An ionic liquid-polyaniline/tungsten disulfide (IL-PANI/WS_2) composite was synthesized in 1-butyl-3-methylimidazole tetrafluoroborate (LB104) aqueous solution by *in-situ* polymerization and characterized by Fourier transform infrared spectroscopy. A current-carrying friction and wear tester was used to study the tribological properties of steel–steel and copper–copper friction pairs lubricated by an IL-PANI/WS_2 lithium complex grease (LCG). After the experiment, scanning electron microscope was used to observe the surface morphology of the wear scar on the steel and copper plates, and X-ray photoelectron spectrometer was used to analyze the elemental composition of the wear scar surface. The results show that compared with greases containing IL-PANI and WS_2, greases containing IL-PANI/WS_2 exhibit better antiwear performance when lubricating steel–steel friction pairs and better tribological performance and electrical conductivity when lubricating copper–copper friction pairs. Therefore, it can be concluded that WS_2 and IL-PANI have a synergistic effect.

Keywords: lithium complex grease (LCG); current-carrying friction; additive; ionic liquid-polyaniline/tungsten disulfide (IL-PANI/WS_2)

1 Introduction

With the development of the mechanical manufacturing industry, friction and wear have become an important form of energy consumption worldwide, accounting for about one-third to one-half of energy consumed. Nearly 50% of mechanical component failures result from wear and friction. It is increasingly important to reduce friction and wear [1]. Layered solid lubricants such as molybdenum disulfide (MoS_2), graphene, and tungsten disulfide (WS_2) are often used as solid or fluid lubricant additives because of their low tangential resistance resulting from the interlayer van der Waals force [2]. However, compared with MoS_2 and graphene, WS_2 has better conductivity and can act as a conductive skeleton. Moreover, it is compatible with most oils and greases, has better compatibility, and can maintain the hydrodynamic layer. Finally, tungsten disulfide is nontoxic, noncorrosive, and inert. Compared with bulk tungsten disulfide, micro-/nanoparticle tungsten disulfide can not only be used as a conventional additive, but also has excellent tribological properties under harsh conditions such as high temperature and high load. Therefore, the preparation and modification of nanosize tungsten disulfide have attracted considerable attention. Zhang et al. [3] reported that the tribological properties of WS_2 nanorods as a lubricating oil additive are better than those of 2H-WS_2 lubricating oil. The rolling effect between friction surfaces and the physical friction film formed on the substrate can explain the good friction and wear properties of WS_2 nanorods. Since the discovery of fullerene-like tungsten disulfide (IF-WS_2) [4], many researchers have demonstrated that it shows excellent antifriction and wear resistance in synthetic oil, mineral oil, and vegetable oil because of its unique

* Corresponding author: Yanqiu XIA, E-mail: xiayq@ncepu.edu.cn

spherical structure and material characteristics [5–7]. Ouyang et al. [7] added oleic-acid-modified IF-WS_2 nanoparticles to castor oil. The mixed lubricant had excellent tribological properties, and the improved lubrication performance was attributed to the polarity of castor oil and the unique bearing structure and dispersion stability of modified IF-WS_2. Castor oil molecules are better adsorbed around modified IF-WS_2 to form a friction oil film in heavy-duty bearings. Zhang et al. [8] used 1-methyl-2,4-bis(n-octadecylurea) benzene (MOB) and WS_2 nanosheets as lubricate additives. The fixed function groups of MOB prevent the aggregation and precipitation of WS_2 nanosheets, resulting in enhanced tribological properties. Jiang et al. [9] studied ultrathin WS_2 nanosheets modified by oleamine as a poly-α-olefin additive; they exhibited good dispersion stability and excellent lubrication performance in a wide temperature range.

Many recent studies have also reported that layered solid lubricants modified by metals or metal oxides have enhanced tribological properties. MoS_2 has been modified by metals or metal oxides such as Ni, Cu, Fe_3O_4, Al_2O_3, and ZnO [10–14]. Ag-, Cu-, and ZnO-modified graphene also exhibits enhanced tribological properties when a lubricant additive is used [15–17]. Lu et al. [18] prepared a WS_2/TiO_2 composite. Although it had little effect on the antifriction effect of diisooctyl sebacate (DOS), it significantly improved the wear resistance of DOS, indicating a synergistic lubrication effect of WS_2 and TiO_2. Xu et al. [19] used a novel biomimetic surface modification method based on the mussel-inspired chemical synthesis of WS_2–polydopamine–methoxypolyethylene glycol amine. After modification, the dispersion stability of the modified WS_2 nanosheets in polyalkylene glycol (PAG) was significantly improved, and they had better antifriction and antiwear performance than WS_2 in PAG base oil. These findings indicate that the layered solid is modified mainly by chemical reagents, metals, or metal oxides, and few polymer-modified laminate solid additives have been studied. Polyaniline (PANI) has the advantages of easy synthesis, good corrosion resistance, and excellent tribological properties, and its conductivity can be controlled by doping with organic or inorganic acids at different concentrations. It is a conductive lubricating polymer with broad application prospects [20, 21]. Ionic liquids (ILs) are electrically conductive, flammable, and thermally stable, and they have very low vapor pressures. They participate in various intermolecular interactions, such as the Coulomb, van der Waals, dispersion, n–p and p–p interactions and hydrogen bonding, by which they can dissolve organic, inorganic, and polymeric materials; they are considered as green alternatives to volatile organic solvents [22]. The chemical polymerization of PANI in ILs is expected to be useful for reducing the charge transfer resistance and improving the conductivity [23]. Our previous research demonstrated that IL-modified PANI has excellent tribological properties, corrosion resistance, and electrical conductivity. It can effectively reduce the volume and surface resistance of greases, reduce the contact resistance, and ensure that the friction state is stable [24–26]. In addition, we have prepared electrical compound greases with excellent conductivity and tribological properties by using conductive additives such as carbon nanotubes, lithium salt, ILs, and conductive PANI. The composite grease can protect the contact area in transmission lines, prevent the corrosion of metal devices, reduce the contact resistance between circuit contacts, and improve the quality of electrical contacts [27].

To investigate whether there is a synergistic effect between PANI and WS_2, an IL-PANI/WS_2 composite additive was synthesized by *in-situ* polymerization in an aqueous solution containing the IL 1-butyl-3-methylimidazole tetrafluoroborate as the solvent. Then, the tribological and conductive properties of IL-PANI/WS_2 as a lithium complex grease (LCG) additive were investigated. Finally, models of the lubrication and conductive mechanisms are proposed.

2 Experimental

2.1 Materials

Poly-α-olefin (PAO40) was purchased as a base oil from China Petroleum Lube Company; it has kinematic viscosities of 396 mm^2/s at 40 °C and 39 mm^2/s at 100 °C. Lithium hydroxide, 12-hydroxyglycanic acid, sebacate, and acetone were purchased from China Pharmaceutical Group Chemical Reagent Co., Ltd.

Tungsten disulfide powder (particle size: 5 μm) was purchased from Jiangsu Xianfeng Nano-material Technology Co., Ltd., China. Aniline (Ani), ammonium persulfate (APS), and 1-butyl-3-methylimidazole tetrafluoroborate (LB104, purity: 97%) were purchased from Shanghai Macklin Biochemical Technology Co., Ltd., China.

2.2 Synthesis and characterization of IL-PANI/WS_2 composite

Figure 1 shows a schematic diagram of the IL-PANI/WS_2 composite preparation process. First, 6.99 g of LB104 was added to 300 mL of deionized water, and the mixture was stirred for 1 h for complete dissolution. Second, 0.31 g of tungsten disulfide powder was ground with a mortar for 6 h. A certain amount of the powder was added to a 0.1 mol/L LB104 solution, dispersed for 30 min by ultrasonication, and stirred until a uniform solution was obtained. Subsequently, 2.79 g of aniline monomer was added, and additional tungsten disulfide powder was added under continuous stirring; the mixture was stirred for 1 h for complete dissolution. Third, 6.9 g of APS powder was mixed into 100 mL of deionized water, and ultrasonic dispersion was used to prepare an APS aqueous solution. This solution was added dropwise to an LB104 solution containing the aniline monomer, which was stirred continuously and reacted for 10 h. Finally, suction filtration was applied after the reaction, and the product was rinsed with absolute ethanol and deionized water until the filtrate was colorless. The product was then dried in an oven for 24 h.

Finally, the product was dissolved in a mortar with petroleum ether and ground for 2 h to prepare dark green IL-PANI/WS_2 powder. The synthetic steps of IL-PANI are consistent with the above method. Table 1 lists the quantity of each substance used to synthesize the composite material. The composite material was characterized by Fourier transform infrared (FTIR) spectroscope (Nicolet iS10, Thermo Scientific, USA). IL-PANI/WS_2 with a mass fraction of 10% tungsten disulfide is denoted as PW10, whereas that with a mass fraction of 30% tungsten disulfide is denoted as PW30.

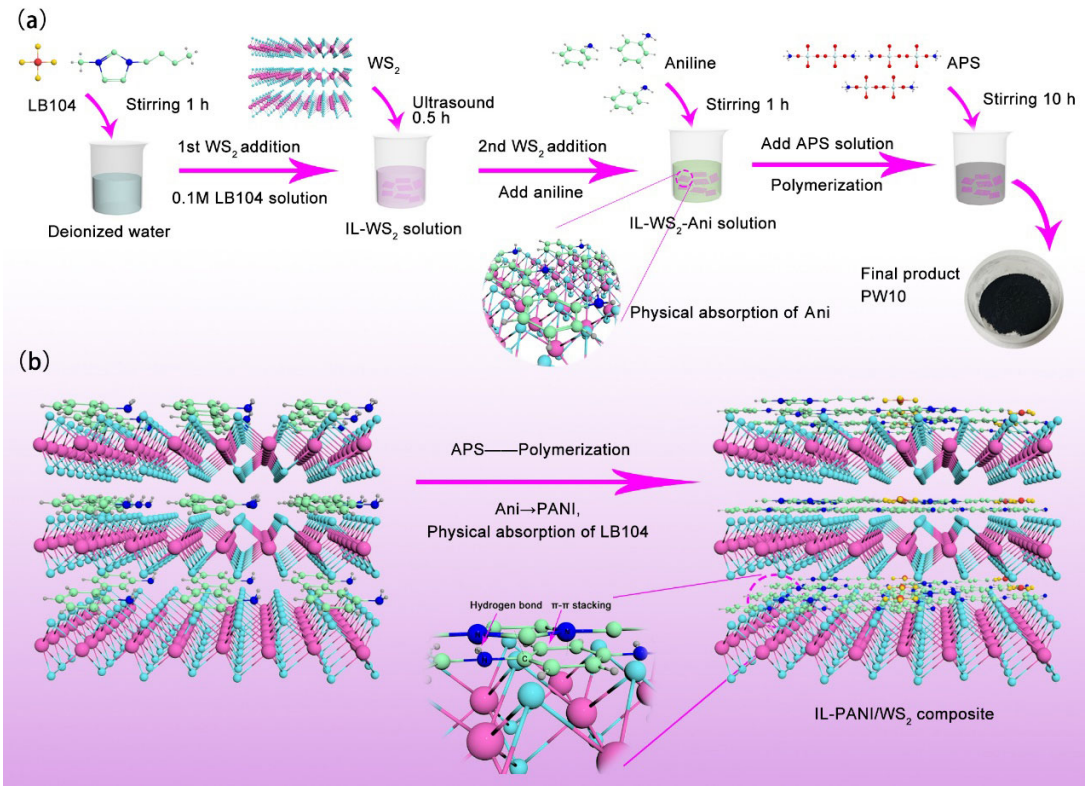

Fig. 1 (a) Schematic illustration of synthesis of IL-PANI/WS_2 composite (PW10). (b) Polymerization mechanism of aniline on surface of WS_2 in LB104 solution.

Table 1 Quantity of each substance used in composite synthesis.

Sample	*c*(Ani)/*c*(APS)	*c*(LB104) (mol/L)	*c*(Ani) (mol/L)	*m*(LB104) (g)	*m*(Ani) (g)	*m*(WS_2) (g)	*m*(APS) (g)
IL-PANI	1:1	0.1	0.1	6.99	2.79	0	6.9
PW10	1:1	0.1	0.1	6.99	2.79	0.31	6.9
PW30	1:1	0.1	0.1	6.99	2.79	1.49	6.9

2.3 Synthesis and characterization of IL-PANI/WS_2 greases

The LCG was synthesized according to Ref. [25]. Briefly, 12-hydroxy alkyl stearic acid (7.87%) was added to a beaker containing PAO40, heated to 80 °C, and stirred until it dissolved completely. A measured lithium hydroxide solution was added, and the remaining PAO40 (38%), sebacic acid (2.11%), and aqueous lithium hydroxide (0.9%) were added sequentially to the beaker. which was held for 10 min at 210 °C. After cooling to 80 °C, the prepared additive was added to the beaker under continuous stirring. After cooling to room temperature, the greases containing the additive were obtained by passing the mixture three times through a three-roll mill.

The volume resistance of the lubricating greases with the added composite materials was measured using a volume surface tester (GEST-121, Beijing Guance Jingdian Instrument Equipment Co., Ltd., China), and the volume resistivity was calculated according to the equation $\rho_v = R_x \frac{A}{h}$ (where ρ_v is the volume resistivity, R_x is the volume resistant, A is electrode effective area, h is specimen thickness). A loop resistance tester (HLY-200a, Beijing Guance Instrument Equipment Co., Ltd., China) was used to measure the contact resistance of the grease at a bolt tightening torque of 10 N·m, energizing current of 100 A, and energizing time of 10 s. The effects of the additives on the dropping point and corrosion properties of the lubricating grease were tested according to the national standards GB/T 4929 and GB/T 7326, respectively. The lubricating grease was applied evenly to a polished copper strip and held at a constant temperature of 100 °C for 24 h. After the test, the copper strip was cleaned using petroleum ether and compared with the copper strip corrosion standard color card to obtain the corrosion grade of the lubricating grease containing additives.

2.4 Tests of tribological and conductive properties

To investigate the tribological properties of IL-PANI/WS_2 as an additive in LCG, tribological tests were conducted using a reciprocal tribometer (MFT-R4000, State Key Laboratory of Solid Lubrication, Chinese Academy of Sciences, China). The friction pairs were in ball–plate contact form, and the upper and lower parts of the friction pair were both made of GCr15. The steel ball had a diameter of 5 mm and a hardness of 630–636 HV. The dimensions of the steel plate were Ø24 mm × 5 mm, and the hardness was 641 HV. Before and after each experiment, the steel ball and plate were cleaned with an ultrasonic machine for 10 min, and 0.3 g of lubricating grease was evenly applied at the contact point of the friction pair. The experiment for each concentration of each additive was repeated at least three times. In addition, a copper–copper friction pair was also tested using a copper ball (Ø5 mm, hardness: 180 HV) and copper plate (30 mm × 30 mm, hardness: 150 HV). The voltage was 0 V, and the other conditions were the same as in the current-carrying test (see Section 2.4.3).

2.4.1 Investigation of optimal concentration of additives (using PW10 grease as an example)

According to previous studies, the additive concentration is among the most important factors affecting the tribological properties of grease. Under the same experimental conditions, the tribological properties of greases with different concentrations of different additives (single materials and composites) were studied to determine the optimal concentration of each additive. Taking PW10 as an example, the specific experimental conditions were as follows: sample concentration: 1%, 2%, 3%, and 4%; temperature: 25 °C; humidity: 40%; sliding length: 5 mm; frequency: 5 Hz; load: 50 N; and time: 30 min.

2.4.2 Effect of load factor on tribological properties of grease (using PW10 grease as an example)

After the relative optimal concentration of PW10 was determined, the effect of the load factor on the tribological properties of PW10 was investigated by varying the load. The detailed experimental conditions are as follows: load: 25, 50, 100, and 150 N; temperature: 25 °C; humidity: 40%; sliding length: 5 mm; frequency: 5 Hz; and time: 30 min.

2.4.3 Current-carrying performance test of grease

To investigate the conductive properties of IL-PANI/WS_2 as an additive in the LCG, current-carrying tests were conducted on a current-carrying friction and wear tester (MFT-R4000, Fig. 2). The friction pair used ball–plate contact. The diameter of the copper ball was 5 mm, and the hardness was 180 HV. The dimensions of the copper plate were 30 mm × 30 mm, and the hardness was 150 HV. Before and after each experiment, the copper ball and plate were cleaned using an ultrasonic machine for 10 min, and 0.3 g of lubricating grease was evenly applied at the contact point of the friction pair. The experiment for each concentration of each additive was repeated at least three times.

After the relative optimal concentrations of different additives (single materials and composites) were determined, the test was conducted under the following experimental conditions: voltage: 1.5 V; load: 15 N; temperature: 25 °C; humidity: 40%; sliding length: 5 mm; frequency: 2 Hz; and RT: 30 min.

2.5 Characterization of worn surfaces

After the tribological tests, the steel plate was ultrasonicated for 30 min. Then, the width of the grinding area was measured using an optical microscope, and the surface morphology of the grinding surface was observed using scanning electron microscope (SEM; EVO-18, Zeiss, Germany). X-ray photoelectron spectrometer (XPS; PHI-5702, Physical Electronics Company, USA) was used to determine the chemical states of the typical elements on the rubbing surfaces. A carbon binding energy of 284.6 eV was used as a reference, and the pass energy was 29.3 eV, with a resolution of approximately ±0.3 eV.

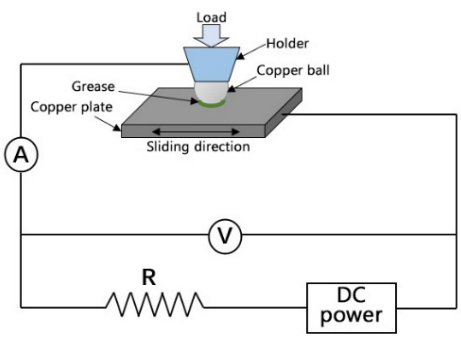

Fig. 2 Schematic of current-carrying friction test.

3 Results and discussion

3.1 Characterization results

Figure 3 shows the FTIR spectra of the composites. The characteristic peaks at 3,170 and 2,960 cm^{-1} are related to the H–C–C–H bond asymmetric stretching vibration and N=C bond stretching vibration on the imidazole ring, respectively [28]. The peak at 1,654 cm^{-1} indicates C=O group stretching. The peaks at 1,560 and 1,478 cm^{-1} are attributed to C=C bond stretching vibrations in the quinone and benzene ring structures, respectively [29]. The ratio of benzenoid to quinoid rings is larger than 1.0, indicating that IL-PANI and PW30 are in the intermediate oxidation state [26]. The peaks near 1,298 and 1,230 cm^{-1} indicate C–N bond stretching [30]. The peaks at 1,111 and 796 cm^{-1} are assigned to in-plane and out-of-plane bending vibrations, respectively, of the C–H bond on

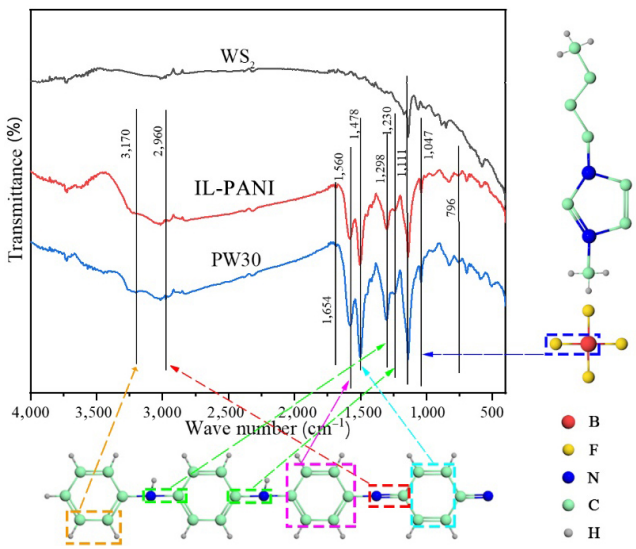

Fig. 3 FTIR characterization of composites.

1,4-disubstituted rings [31]. The characteristic peak at 1,047 cm^{-1} is attributed to B–F bond stretching vibration of anions in the IL LB104 [32]. These peaks demonstrate that IL-PANI and PW30 were successfully prepared.

3.2 Physical and chemical properties of greases

Table 2 shows the physical and chemical properties of the greases. The greases containing additives have higher dropping points than the base grease, because both tungsten disulfide and PANI have large specific surface areas, which hinder the flow of liquid molecules. The volume resistivity and contact resistance show the same tendency, decreasing in the order of LCG > 4% WS_2 > 4% IL-PANI > 4% PW10 > 4% PW30. This result reflects the improved conductivity of PW10 and PW30. The copper strip corrosion grade is 1a, indicating that the four additives do not affect the corrosion grade of the LCG.

3.3 Tribological test results

3.3.1 Results of steel–steel friction without current-carrying

Figure 4 shows that when IL-PANI is used as an LCG additive, the coefficient of friction (COF) first decreases and then increases with increasing IL-PANI concentration, and the variation in wear width shows the same trend. According to the COF and wear width results, the optimal IL-PANI concentration in the LCG is 2%. When WS_2 is used as an LCG additive, the COF does not change significantly and is lower than that of the base grease. At an additive concentration of 3%, the COF shows slight improvement. The COF and wear width results indicate that the antiwear effect of WS_2 is the greatest at a concentration of 3%. Therefore, the optimal WS_2 concentration is 3%. As shown in Fig. 4(b), the antiwear performance of greases containing the composites PW10 and PW30 is significantly better than that of composites containing IL-PANI or WS_2, and the optimal concentration of the two composites is 2%. Thus, 2% IL-PANI, 3% WS_2, 2% PW10, and 2% PW30 were selected for the variable load experiment and current-carrying friction test.

Figure 5 shows the average COFs and wear widths of the steel plate under different loads at the optimal additive concentrations. Each additive decreases the COF and wear width of the LCG. The COF and wear width increase with increasing load. At 25 N, IL-PANI has the lowest COF. As the load increases, the friction reduction effect of IL-PANI gradually decreases,

Table 2 Physical and chemical properties of greases.

Sample	LCG	4% WS_2	4% IL-PANI	4% PW10	4% PW30
Dropping point (℃)	235	274	267	269	271
Volume resistivity (Ω·cm)	3.40×10^{11}	3.21×10^{11}	2.91×10^{11}	1.90×10^{11}	7.90×10^{10}
Contact resistance (μΩ)	29.3–29.5	28.9–29.0	28.6–28.7	27.4–28.0	27.1–27.2
Anticorrosion grade of copper sheet	1a	1a	1a	1a	1a

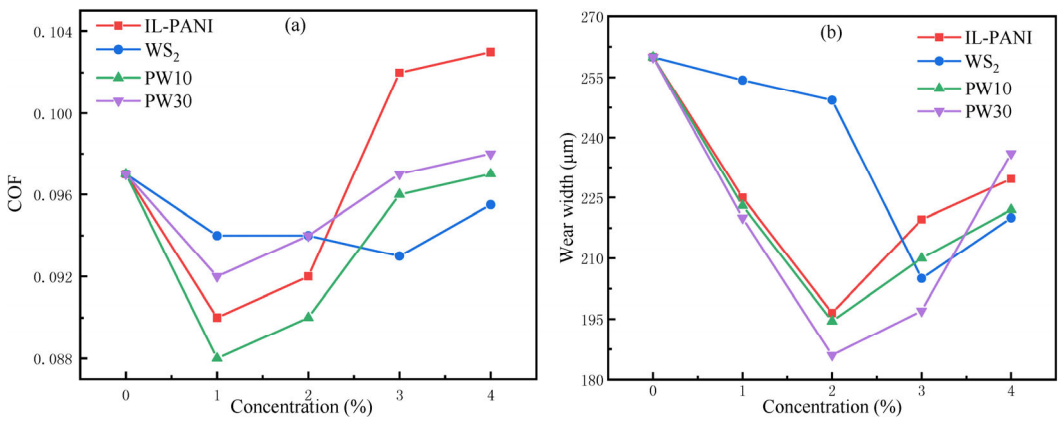

Fig. 4 (a) COFs and (b) wear widths of various greases with different additive concentrations (voltage: 0 V; load: 50 N; frequency: 5 Hz; stroke: 5 mm).

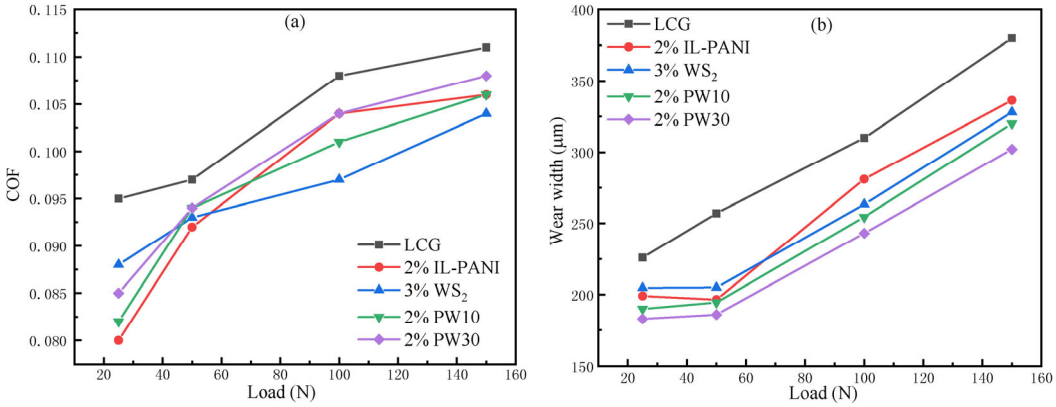

Fig. 5 (a) COFs and (b) wear widths of greases with optimal additive concentrations (voltage: 0 V; load: variable; frequency: 5 Hz; stroke: 5 mm).

whereas the excellent friction reduction effect of WS_2 is evident at high loads because the structure allows easy slip between layers. Under high load conditions, the wear width increases as follows: PW30 < PW10 < WS_2 < IL-PANI < LCG, which indicates that the greases doped with 2% PW10 and PW30 exhibited excellent antiwear properties.

3.3.2 *Results of copper–copper friction without current-carrying*

As shown in Fig. 6(a), the COF of the copper–copper friction pair under non-current-carrying conditions exhibits complex variation. The grease containing 3% WS_2 has the lowest COF on the copper–copper friction pair; the COFs then follow the order: PW10 < PW30 < IL-PANI < LCG. However, with increasing friction time, the antifriction effects of PW10 gradually improve, and the COF is lower than that of the grease with 3% WS_2. The wear width results (Fig. 6(b)) show that IL-PANI has the strongest antiwear effect on the copper–copper friction pair under non-current-carrying conditions, and the wear spot width increases in the following order: IL-PANI < WS_2 < LCG < PW10 < PW30. The antiwear effects of the four additives in the LCG on the copper–copper pair are completely different from those on the steel–steel friction pair. The reason may be that the surface hardness of the steel plate used in the test is 3.5 times that of the copper plate.

3.4 Current-carrying test results

As shown in Fig. 7(a), all the greases containing additives show better friction reduction performance than the LCG. The grease with 2% PW30 has the lowest COF, and the COF increases in the following order: PW30 < PW10 < IL-PANI < WS_2 < LCG. Figure 7(b) shows the wear width of the copper plate lubricated

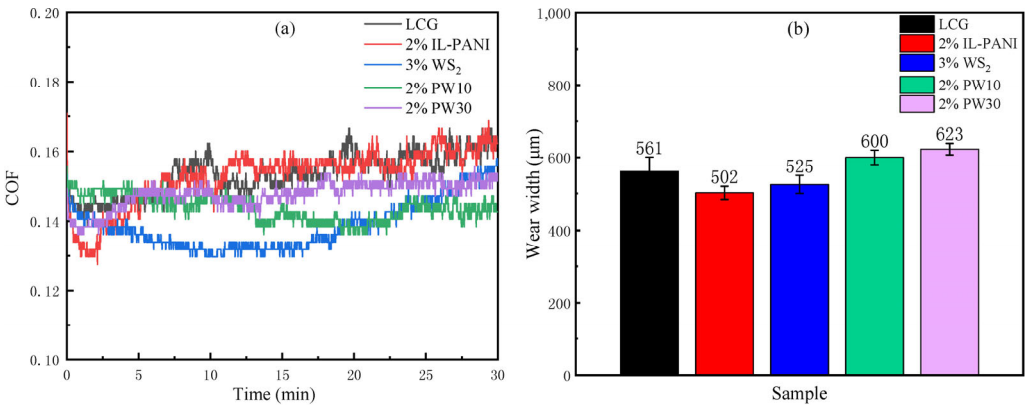

Fig. 6 (a) COFs and (b) wear widths of greases with optimal additive concentrations on copper–copper friction pair (voltage: 0 V; load: 15 N; frequency: 2 Hz; stroke: 5 mm).

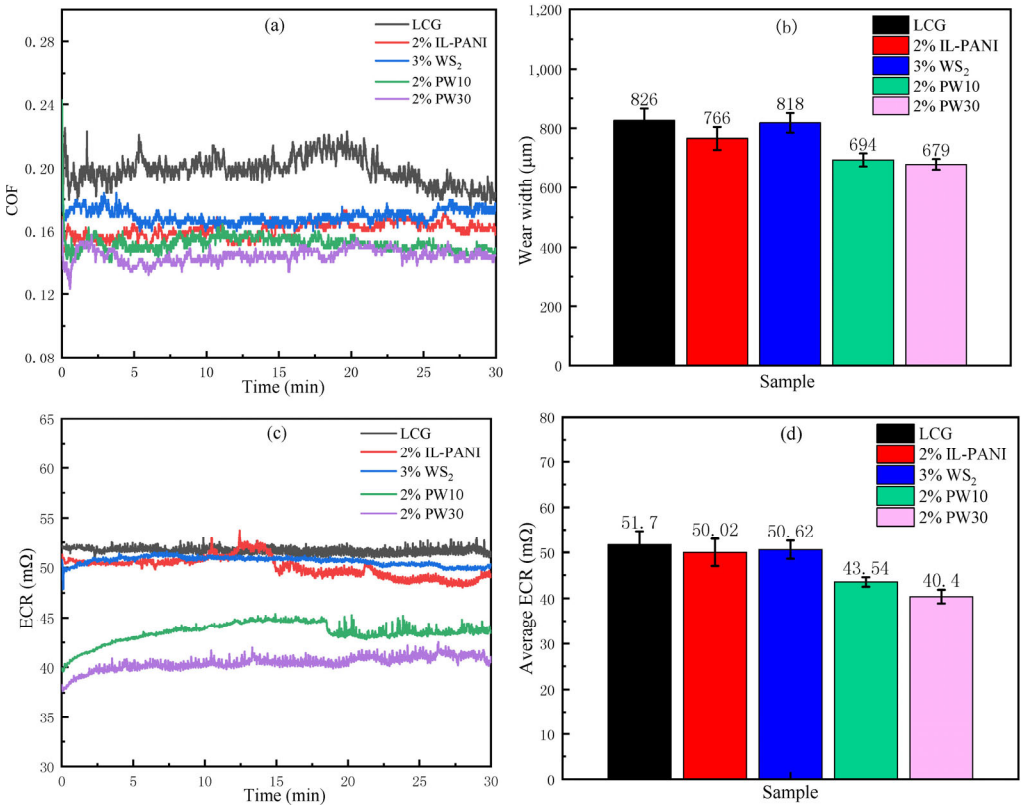

Fig. 7 (a) COFs, (b) wear widths, (c) ECRs, and (d) average ECRs of greases with optimal additive concentrations on copper–copper friction pair (voltage: 1.5 V; load: 15 N; frequency: 2 Hz; stroke: 5 mm).

by greases containing different additives. All four additives clearly reduce the wear width. The wear width increases in the same order as the COF, indicating that PW30 exhibits the best antiwear performance. This result indicates that the synergistic effect and tribological properties improve with increasing WS_2 content in the PANI/WS_2 composite. Figure 7(c) shows the electrical contact resistance (ECR) versus time. The 2% PW30 grease has the smoothest contact resistance curve, and the contact resistance of the 3% WS_2 grease also shows little fluctuation. Figures 7(a) and 7(c) show that the 2% PW30 grease has the best tribological performance and most stable contact resistance. As shown in Fig. 7(d), the average contact resistance increases in the following order: PW30 < PW10 < IL-PANI < WS_2 < LCG. This result reflects the synergistic effect of IL-PANI and WS_2 on the conductivity. With increasing WS_2 molar ratio, the contact resistance of the composite decreases, which is consistent with the results of volume surface resistivity measurement (Table 2), and PW30 shows the lowest contact resistance.

3.5 SEM analysis of worn surfaces

3.5.1 Worn surfaces of steel–steel friction pair without current-carrying

Figure 8 shows SEM images of the steel plate surface after lubrication with the greases at 150 N. Figures 8(a) and 8(b) show that after LCG lubrication, the scratches on the wear spots appear at low magnification are obvious, and scratches and larger pits are clearly visible at high magnification. These results show that the LCG has a poor lubricating effect. Figures 8(c) and 8(d) show that after lubrication by the 2% IL-PANI grease, shallow scratches appear at high magnification, but uneven pits are visible, indicating that IL-PANI has some antiwear effect as an additive. Figures 8(e) and 8(f) show that after lubrication by the 3% WS_2 grease, scratches are not obvious, but pits are visible under high magnification. As shown in Figs. 8(g) and 8(h), after lubrication by the 2% PW10 grease, the lubrication effect is significantly improved. Wear spots and scratches are faintly visible, but no obvious scratches or pits appear under high

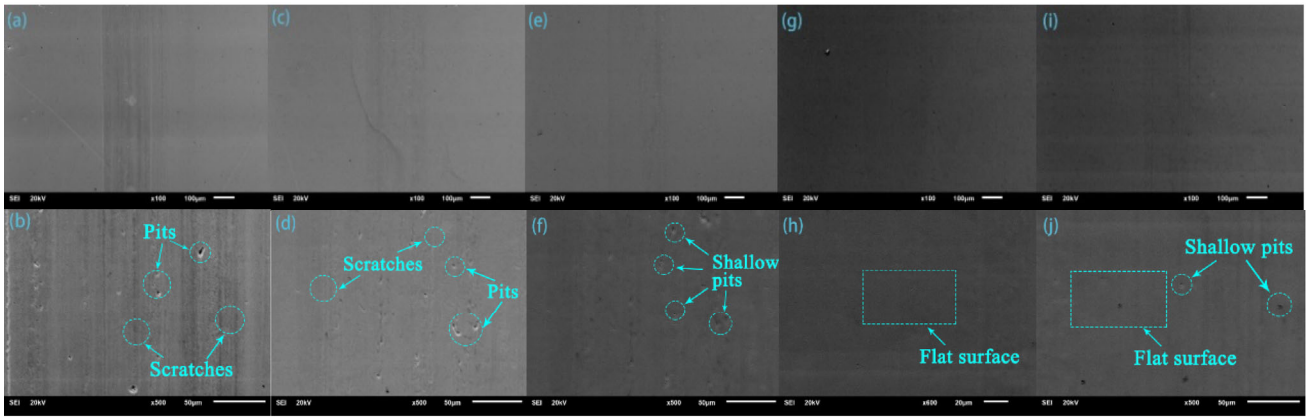

Fig. 8 SEM images of steel plate surfaces lubricated with different greases: (a, b) LCG, (c, d) 2% IL-PANI, (e, f) 3% WS_2, (g, h) 2% PW10, and (i, j) 2% PW30 (voltage: 0 V; load: 150 N; frequency: 5 Hz; stroke: 5 mm).

magnification, and the surface is extremely flat. Compared with that after lubrication by the 2% IL-PANI grease and 2% WS_2 grease, the wear spot morphology is greatly improved. Figures 8(i) and 8(j) show that after lubrication by the 2% PW30 grease, the scratches on the wear spots are not obvious, and only a few shallow pits appear at high magnification, indicating that PW30 also has an excellent effect on the lubrication performance. When the PW10 and PW30 composites were used as LCG additives, the results demonstrate that PANI and WS_2 have a synergistic effect on the antiwear properties.

3.5.2 Worn surfaces of copper–copper friction pair with current-carrying

Figure 9 shows SEM images of the copper plate surface lubricated with different greases under current-carrying conditions. Figures 9(a) and 9(b) show multiple large, wide furrows on the wear surface after lubrication with the LCG. At high magnification, the furrows are clearly visible, wide, and deep, indicating that the LCG has a poor lubricating effect on the copper plate. Figures 9(c) and 9(d) show that the wear spot surface is flat after lubrication with the 2% IL-PANI grease, but shallow furrows appear at high magnification, indicating that IL-PANI has some antiwear effect as a conductive additive. Figures 9(e) and 9(f) show that after lubrication with the 3% WS_2 grease, the scratches on the wear spots at low magnification are slightly deeper than those after lubrication with the 2% IL-PANI grease, and dense shallow furrows appear at high magnification. These results show that the performance of the 3% WS_2 grease is inadequate under current-carrying conditions. Figures 9(g) and 9(h) show that the 2% PW10 grease exhibits a significantly improved lubrication effect.

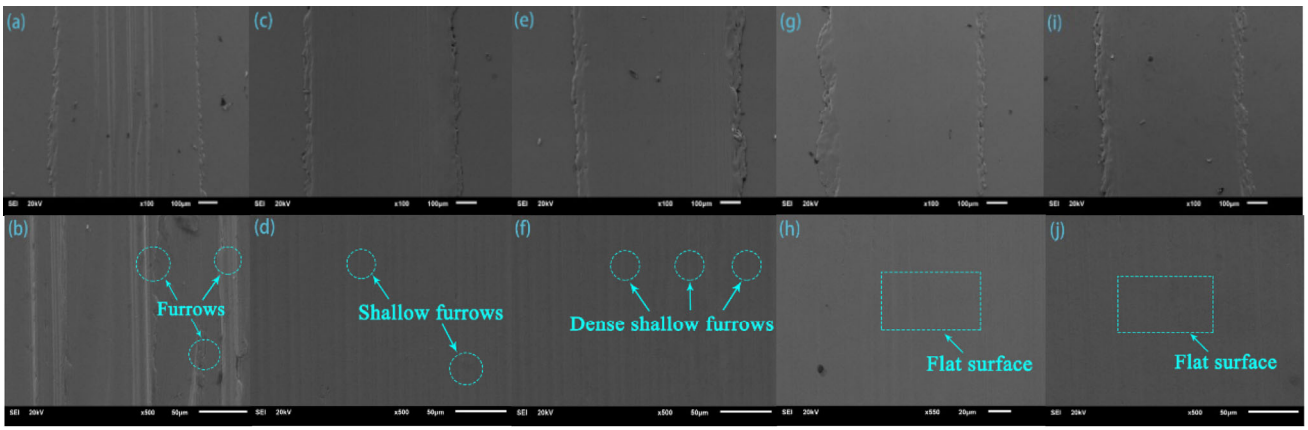

Fig. 9 SEM images of copper plate surfaces lubricated with different greases: (a, b) LCG, (c, d) 2% IL-PANI, (e, f) 3% WS_2, (g, h) 2% PW10, and (i, j) 2% PW30 (voltage: 1.5 V; load: 15 N; frequency: 2 Hz; stroke: 5 mm).

At low magnification, the wear spot surface is extremely flat except at the edge. No obvious furrows or pits appear at high magnification, and the surface is extremely flat. Compared with that after lubrication with the 2% IL-PANI and 3% WS_2 greases, the wear spot morphology is greatly improved. As shown in Figs. 9(i) and 9(j), after lubrication with the 2% PW30 grease, the scratch on the wear spot is flat, and the worn surface is smoother than those after lubrication by the other four greases at high magnification. This result shows that the 2% PW30 grease also exhibits excellent lubrication performance. Therefore, when the PW10 and PW30 composites were used as LCG additives, the results demonstrated that PANI and WS_2 also have a synergistic effect on the antiwear performance under current-carrying conditions.

3.6 XPS analysis of worn surfaces

Figure 10 shows the XPS spectra of the worn surfaces on the steel and copper plates. The characteristic Fe $2p_{3/2}$ and Fe $2p_{1/2}$ peaks at 711.4 and 725.1 eV in Fig. 10(a) correspond to Fe_2O_3 and FeO, respectively [33, 34]. Similarly, the Cu 2p spectra (Fig. 10(b)) clearly show $2p_{1/2}$ and $2p_{3/2}$ peaks at 952.1 and 932.4 eV, respectively, with peak splitting of 19.7 eV, in good agreement with the standard separation of Cu. According to Refs. [35, 36], curve fitting of the Cu $2p_{3/2}$ region shows three copper species with binding energies of 933.6, 934.8, and 932.5 eV, which are assigned to CuO, $Cu(OH)_2$, and Cu_2O or Cu metal, respectively. As shown in Figs. 10(c) and 10(d), the W 4f spectra exhibit two main peaks, W $4f_{7/2}$ and W $4f_{5/2}$ (resulting from spin–orbit splitting), at 32.5 and 34.6 eV, respectively, which correspond to WS_2. Additionally, a small amount of oxidized tungsten (37.4 eV) is also detected, indicating that WO_3 was generated on the surface of the steel plate [37, 38]. As shown in Fig. 10(e), the peaks at 529.7 and 530.6 eV may belong to O–Fe compounds and WO_3, respectively, whereas the peak at 533.5 eV in the O 1s spectra in Fig. 10(f) may belong to C–O compounds or pollutants [39]. In Fig. 10(f), the O 1s peaks of the copper plate show the same elements as those in Fig. 10(b). In Fig. 10(g), the peaks at 170.2 and 171.4 eV in the S 2p spectra correspond to S $2p_{3/2}$ and S $2p_{1/2}$, respectively, indicating the presence of SO_4^{2-}, and the O 1s binding energy is 533.2 eV in Figs. 10(e) and 10 (f), indicating the presence of $FeSO_4$ on the steel surface and $CuSO_4$ on the copper surface [35]. This result indicates that the sulfur in WS_2 reacts with the surface of the friction pair during friction. In Fig. 10(h), the F 1s peaks at approximately 685.5 and 684.6 eV may correspond to FeF_2 and FeF_3, respectively, on the worn steel surface. However, no characteristic peak appears on the surface of the copper plate, and BF_4^- does not react with the copper surface in combination with boron [26, 39]. The peak values of XPS peaks not mentioned above but fitted in Fig. 10 were obtained by retrieving the results for the corresponding elements from the National Institute of Standards and Technology XPS database, USA.

3.7 Lubrication and conductivity mechanisms

The excellent tribological properties of IL-PANI/WS_2 as an LCG additive may result from the lubrication mechanisms of the IL, PANI, and tungsten disulfide. Figure 11 shows schematic illustrations of the lubrication and conduction mechanisms.

The lubrication mechanism of IL-PANI as an additive includes physical adsorption and chemical reaction between the IL and PANI [26]. ILs very easily form adsorption films on a friction surface, including physical adsorption and chemical reaction films. The escape of low-energy electrons from the metal surface fills the metal surface with electron-rich groups, and the anions in the IL are adsorbed on the contact surface by electrostatic attraction. The cations in the IL accumulate on the contact surface because of anion attraction; the resulting protective film on the contact surface [40] reduces the probability of direct contact of the friction pair. In addition, during the friction process, the active fluorine in the IL reacts with the contact surface to generate FeF_2 and FeF_3, whereas most of the boron is physically adsorbed [24]. When the chemical reaction film reaches a balance between formation and wear, it can effectively reduce the antiwear and antifriction performance in the contact area. Then, PANI particles hinder the direct contact of the friction pair, act as a bearing, and form a lubricating film that is easily sheared. In addition, nitrogen-containing compounds are generated in the friction process, which improve the tribological properties of the friction pair [27]. Tungsten disulfide

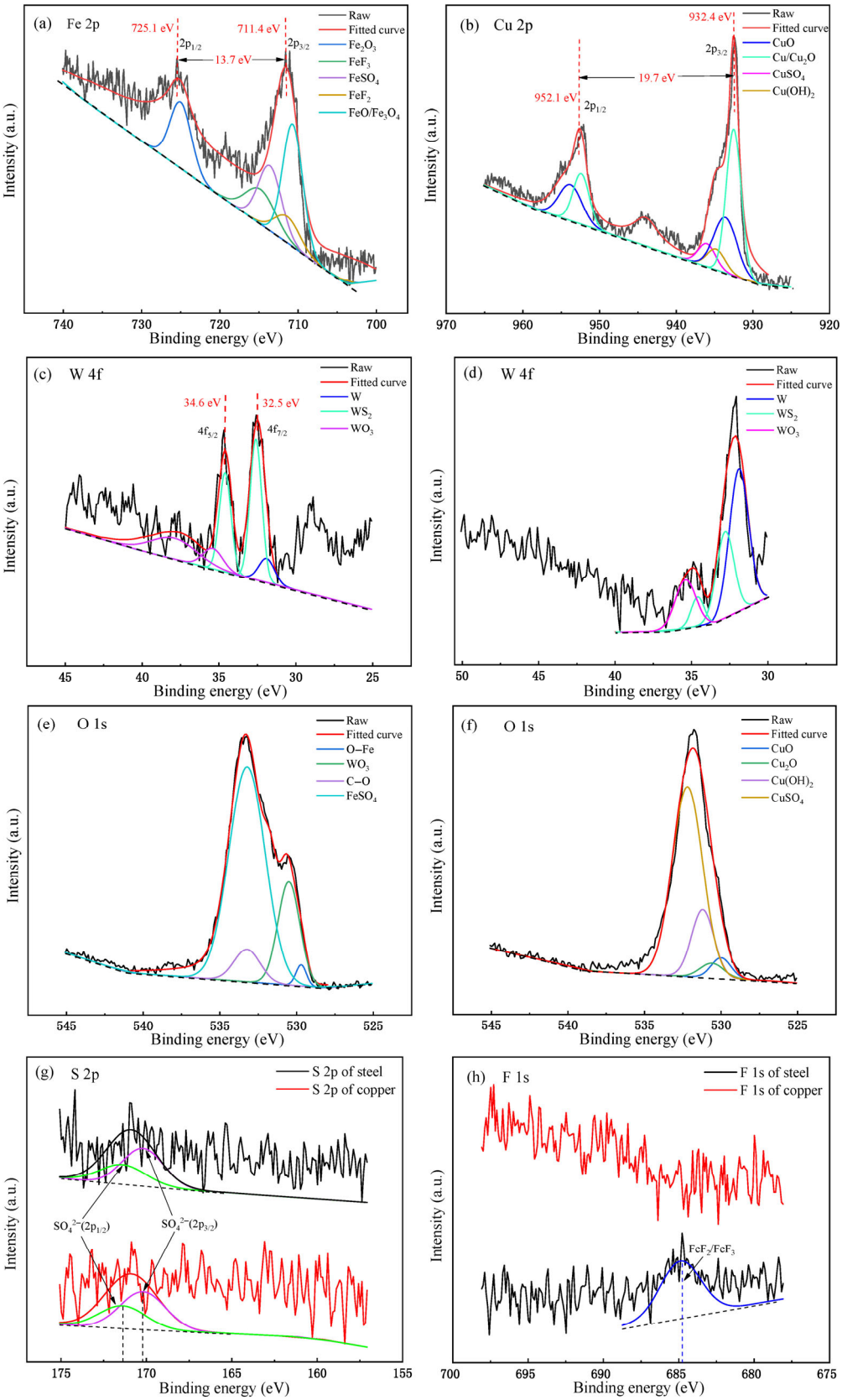

Fig. 10 XPS spectra of elements on wear surface of plate lubricated by LCG + 2% PW10: (a) Fe 2p, (b) Cu 2p, W 4f for (c) steel plate and (d) copper plate, O 1s for (e) steel plate and (f) copper plate, (g) S 2p, and (h) F 1s.

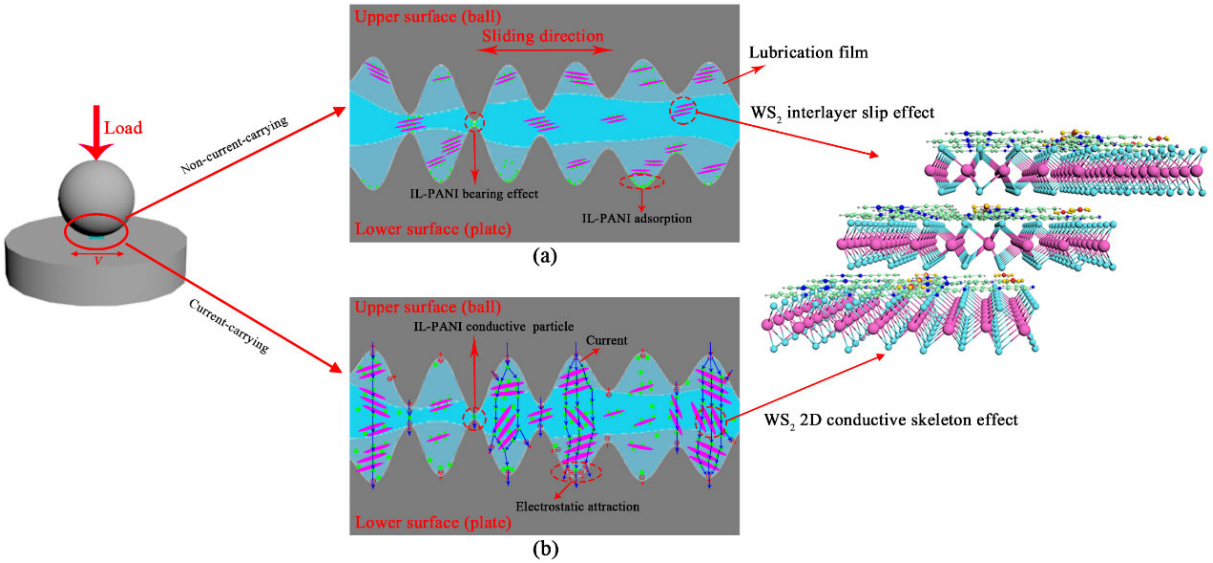

Fig. 11 Schematic illustrations of (a) lubrication mechanism and (b) conduction mechanism of IL-PANI/WS_2 as an additive in grease during friction experiments.

improves the antifriction performance of the LCG because it easily slips between layers, has a large specific surface area, and is easy adsorbed. Sulfur and tungsten compounds can be generated by frictional heating, resulting in friction films with high hardness and excellent wear resistance [37]. However, when IL-PANI alone is used as an additive, abrasive wear increases with increasing IL-PANI content, which decreases the antifriction effect. By contrast, the PW10 and PW30 composites play a buffering role during friction because of the addition of WS_2; consequently, they reduce wear and exhibit excellent antifriction performance.

The improved conductivity of the composite materials can be attributed to two factors. First, ILs are entirely composed of ions and thus have excellent conductivity compared with common organic additives [40]. In imidazole ILs, the second hydrogen ion on the imidazole ring is easily ionized to form free hydrogen ions; then PANI can be added during the reaction to form conductive PANI particles [26]. Second, the conductive macromolecules with conjugate π bonds in PANI inserted into the main intermediate layer of WS_2 have a layered arrangement, which is advantageous for electron transfer between organic and inorganic components [29, 41]. The prepared composites contain the same amount of PANI; WS_2 acts as an excellent two-dimensional (2D) conductive skeleton and provides a direct path for electrons. The layered structure of the PANI/WS_2 composite provides a larger contact surface area; thus, the prepared powder has better electrical conductivity. According to the percolation theory and tunneling effect, when it is added to the LCG, the contact resistance in the current-carrying friction process is lower [27].

4 Conclusions

IL-PANI/WS_2 composites were synthesized by *in-situ* polymerization, and the composite material was added to LCG to enhance its tribological and conductive properties. The conclusions are summarized as follows:

1) In the steel–steel friction pair, the optimal concentration of PW10 and PW30 in the LCG is 2% under the non-current-carrying condition. Furthermore, tribological experiments showed that compared to IL-PANI and WS_2, PW10 and PW30 improve the tribological properties to a certain extent.

2) Under the current-carrying condition for the copper–copper friction pair, the addition of PW10 and PW30 increases the antiwear resistance and decreases the contact resistance.

3) The good electrical conductivity of the IL-PANI/WS_2 composite material results mainly from the synergistic effect of IL-PANI and WS_2. LB104-doped

PANI particles can improve electron transport, and WS_2 acts as a conductive skeleton that provides conductive paths.

4) The improvement in the tribological properties can be attributed to the synergistic effect of physical adsorption and the complex chemical reaction film produced by the composite material on the wear surface during friction. The adsorption of IL-PANI in the friction contact area hinders direct contact of the friction pair. Tungsten disulfide increases the strength of the friction film and generates the interlayer slip, reducing the COF and improving the antifriction properties.

References

[1] Ouyang T C, Shen Y D, Yang R, Liang L Z, Liang H, Lin B, Tian Z Q, Shen P K. 3D hierarchical porous graphene nanosheets as an efficient grease additive to reduce wear and friction under heavy-load conditions. *Tribol Int* **144**: 106118 (2020)

[2] Gong K L, Wu X H, Zhao G Q, Wang X B. Nanosized MoS_2 deposited on graphene as lubricant additive in polyalkylene glycol for steel/steel contact at elevated temperature. *Tribol Int* **110**: 1–7 (2017)

[3] Zhang L L, Tu J P, Wu H M, Yang Y Z. WS_2 nanorods prepared by self-transformation process and their tribological properties as additive in base oil. *Mater Sci Eng A* **454–455**: 487–491 (2007)

[4] Tenne R, Margulis L, Genut M, Hodes G. Polyhedral and cylindrical structures of tungsten disulphide. *Nature* **360**(6403): 444–446 (1992)

[5] Joly-Pottuz L, Dassenoy F, Belin M, Vacher B, Martin J M, Fleischer N. Ultralow-friction and wear properties of IF-WS_2 under boundary lubrication. *Tribol Lett* **18**(4): 477–485 (2005)

[6] Abate F, D'Agostino V, di Giuda R, Senatore A. Tribological behaviour of MoS_2 and inorganic fullerene-like WS_2 nanoparticles under boundary and mixed lubrication regimes. *Tribol Mater Surf Interfaces* **4**(2): 91–98 (2010)

[7] Ouyang T C, Lei W W, Tang W T, Shen Y D, Mo C L. Experimental investigation of the effect of IF-WS_2 as an additive in castor oil on tribological property. *Wear* **486–487**: 204070 (2021)

[8] Zhang R C, Qiao D, Liu X Q, Guo Z G, Cai M R, Shi L. A facile and effective method to improve the dispersibility of WS_2 nanosheets in PAO8 for the tribological performances. *Tribol Int* **118**: 60–70 (2018)

[9] Jiang Z Q, Zhang Y J, Yang G B, Yang K P, Zhang S M, Yu L G, Zhang P Y. Tribological properties of oleylamine-modified ultrathin WS_2 nanosheets as the additive in polyalpha olefin over a wide temperature range. *Tribol Lett* **61**(3): 24 (2016)

[10] Rajendhran N, Palanisamy S, Periyasamy P, Venkatachalam R. Enhancing of the tribological characteristics of the lubricant oils using Ni-promoted MoS_2 nanosheets as nano-additives. *Tribol Int* **118**: 314–328 (2018)

[11] Jia X H, Huang J, Li Y, Yang J, Song H J. Monodisperse Cu nanoparticles @ MoS_2 nanosheets as a lubricant additive for improved tribological properties. *Appl Surf Sci* **494**: 430–439 (2019)

[12] Zheng X J, Xu Y F, Geng J, Peng Y B, Olson D, Hu X G. Tribological behavior of Fe_3O_4/MoS_2 nanocomposites additives in aqueous and oil phase media. *Tribol Int* **102**: 79–87 (2016)

[13] He J Q, Sun J L, Meng Y N, Tang H J, Wu P. Improved lubrication performance of MoS_2–Al_2O_3 nanofluid through interfacial tribochemistry. *Colloids Surf A Physicochem Eng Aspects* **618**: 126428 (2021)

[14] Wu P R, Kong Y C, Ma Z S, Ge T, Feng Y M, Liu Z, Cheng Z L. Preparation and tribological properties of novel zinc borate/MoS_2 nanocomposites in grease. *J Alloys Compd* **740**: 823–829 (2018)

[15] Wang L, Gong P W, Li W, Luo T, Cao B Q. Mono-dispersed Ag/graphene nanocomposite as lubricant additive to reduce friction and wear. *Tribol Int* **146**: 106228 (2020)

[16] Gan C L, Liang T, Li W, Fan X Q, Zhu M H. Amine-terminated ionic liquid modified graphene oxide/copper

nanocomposite toward efficient lubrication. *Appl Surf Sci* **491**: 105–115 (2019)

[17] Ren B J, Gao L, BotaoXie, Li M J, Zhang S D, Zu G Q, Ran X. Tribological properties and anti-wear mechanism of ZnO@graphene core–shell nanoparticles as lubricant additives. *Tribol Int* **144**: 106114 (2020)

[18] Lu Z Y, Cao Z Z, Hu E Z, Hu K H, Hu X G. Preparation and tribological properties of WS_2 and WS_2/TiO_2 nanoparticles. *Tribol Int* **130**: 308–316 (2019)

[19] Xu Z, Lou W J, Zhao G Q, Zhao Q, Xu N, Hao J Y, Wang X B. Preparation of WS_2 nanocomposites via mussel-inspired chemistry and their enhanced dispersion stability and tribological performance in polyalkylene glycol. *J Dispers Sci Technol* **40**(5): 737–744 (2019)

[20] Chang K C, Lai M C, Peng C W, Chen Y T, Yeh J M, Lin C L, Yang J C. Comparative studies on the corrosion protection effect of DBSA-doped polyaniline prepared from *in situ* emulsion polymerization in the presence of hydrophilic Na^+-MMT and organophilic organo-MMT clay platelets. *Electrochimica Acta* **51**(26): 5645–5653 (2006)

[21] Bhadra S, Khastgir D, Singha N K, Lee J H. Progress in preparation, processing and applications of polyaniline. *Prog Polym Sci* **34**(8): 783–810 (2009)

[22] Pahovnik D, Žagar E, Kogej K, Vohlídal J, Žigon M. Polyaniline nanostructures prepared in acidic aqueous solutions of ionic liquids acting as soft templates. *Eur Polym J* **49**(6): 1381–1390 (2013)

[23] Li X L, Liu Y F, Guo W, Chen J J, He W X, Peng F F. Synthesis of spherical PANI particles via chemical polymerization in ionic liquid for high-performance supercapacitors. *Electrochimica Acta* **135**: 550–557 (2014)

[24] Cao Z F, Xia Y Q, Chen C, Zheng K, Zhang Y. Polyaniline as an additive towards improving tribological properties and anti-corrosion performance of ionic liquids-based greases. *Ind Lubr Tribol* **72**(7): 851–856 (2020)

[25] Cao Z F, Xia Y Q. Corrosion resistance and tribological characteristics of polyaniline as lubricating additive in grease. *J Tribol* **139**(6): 061801 (2017)

[26] Cao Z F, Xia Y Q, Chen C. Fabrication of novel ionic liquids-doped polyaniline as lubricant additive for anti-corrosion and tribological properties. *Tribol Int* **120**: 446–454 (2018)

[27] Hu Y C, Xia Y Q. Conductivity and tribological properties of conductive polyaniline as additives in grease. *J Mech Eng* **53**(21): 109–117 (2017) (in Chinese)

[28] Fan X Q, Wang L P. Ionic liquids gels with *in situ* modified multiwall carbon nanotubes towards high-performance lubricants. *Tribol Int* **88**: 179–188 (2015)

[29] Maqsood M, Afzal S, Shakoor A, Niaz N A, Majid A, Hassan N, Kanwal H. Electrochemical properties of PANI/MoS_2 nanosheet composite as an electrode materials. *J Mater Sci Mater Electron* **29**(18): 16080–16087 (2018)

[30] Arefinia R, Shojaei A, Shariatpanahi H, Neshati J. Anticorrosion properties of smart coating based on polyaniline nanoparticles/epoxy-ester system. *Prog Org Coat* **75**(4): 502–508 (2012)

[31] Ding S H, Mao H, Zhang W J. Fabrication of DBSA-doped polyaniline nanorods by interfacial polymerization. *J Appl Polym Sci* **109**(5): 2842–2847 (2008)

[32] Fan X Q, Wang L P. Highly conductive ionic liquids toward high-performance space-lubricating greases. *ACS Appl Mater Interfaces* **6**(16): 14660–14671 (2014)

[33] Wang K P, Wu H C, Wang H D, Liu Y H, Yang L, Zhao L M. Tribological properties of novel palygorskite nanoplatelets used as oil-based lubricant additives. *Friction* **9**(2): 332–343 (2021)

[34] Zou S Y, Wang H X, Li S N, Lu B, Zhao J X, Cai Q H. Selective oxidation of methanol to dimethoxymethane over iron and vanadate modified phosphotungstate. *Appl Surf Sci* **574**: 151516 (2022)

[35] Gaudin P, Fioux P, Dorge S, Nouali H, Vierling M, Fiani E, Molière M, Brilhac J F, Patarin J. Formation and role of Cu^+ species on highly dispersed CuO/SBA-15 mesoporous materials for SO_x removal: An XPS study. *Fuel Process Technol* **153**: 129–136 (2016)

[36] Baskaran P, Nisha K D, Harish S, Ramesh R, Ikeda H, Archana J, Navaneethan M. Improved electrochemical performance of Cu_2NiSnS_4 hierarchical nanostructures as counter electrode in dye sensitized solar cells. *Mater Lett* **307**: 130946 (2022)

[37] Chen H L, Chen G X, Du P F, Yang X, Shao Y, Tian Z L. Tribology of nano-tungsten disulfide powder as an lubricating additive for lithium grease. *Tribology* **35**(6): 651–657 (2015) (in Chinese)

[38] Zhang D Q, Wang H H, Cheng J Y, Han C Y, Yang X Y, Xu J Y, Shan G C, Zheng G P, Cao M S. Conductive WS_2–NS/CNTs hybrids based 3D ultra-thin mesh electromagnetic wave absorbers with excellent absorption performance. *Appl Surf Sci* **528**: 147052 (2020)

[39] Cai M R, Zhao Z, Liang Y M, Zhou F, Liu W M. Alkyl imidazolium ionic liquids as friction reduction and anti-wear additive in polyurea grease for steel/steel contacts. *Tribol Lett* **40**(2): 215–224 (2010)

[40] Xia Y Q, Han Y, Feng X. The research progress on lubrication and electrical conductivity of ionic liquids. *Tribology* **36**(6): 794–802 (2016) (in Chinese)

[41] Wang J, Wu Z C, Hu K H, Chen X Y, Yin H B. High conductivity graphene-like MoS_2/polyaniline nanocomposites and its application in supercapacitor. *J Alloys Compd* **619**: 38–43 (2015)

Yanqiu XIA. He received his Ph.D. degree in mechanical engineering from Northeastern University, China, in 1999, and was selected as a professor in 2007. He joined the School of Energy Power and Mechanical Engineer, North China Electric Power University, in 2010. His current position is as a professor. His research areas cover the tribology of mechanical and electrical equipment, oil monitoring, and artificial intelligence.

Yuanhui WANG. He got his bachelor's degree in 2020 from North China Electric Power University. He will graduate from the same university in 2023 with master's degree of engineering. His research interests include preparation and tribological performance of conductive lubricating greases.

Chenglong HU. He received his bachelor's degree from Beijing Union University, China, in 2019. He is currently a graduate student at North China Electric Power University. His research interests focus on the preparation of conductive additives and the study of tribological properties.

Xin FENG. She received her Ph.D. degree in systems engineering from Northeastern University, China, in 2007. She joined the School of Energy Power and Mechanical Engineer, North China Electric Power University, in 2010. She is currently an associate professor. Her research areas cover tribology and artificial intelligence.